Assessing the Suitability of Video Imaging for Studying the Dynamics of Nearshore Sandbars in Tideless Beaches

Francesca Ribas, Elena Ojeda, Timothy D. Price, and Jorge Guillén

Abstract—**Nearshore sandbars, an important natural defense mechanism of the beaches, can be monitored using shore-based video systems. Before studying bar dynamics with video images, we must establish the relationship between the real bar positions and the videoed bar positions (detected by the preferential wave breaking on the shallows). This analysis becomes essential in the two studied tideless beaches of Barcelona due to the critical differences with respect to the sites studied previously. Bogatell beach is terraced (without a trough) in more than 50% of the profiles. There, the videoed barlines are a good proxy of the terrace edge position. In La Barceloneta beach, with dominance of barred profiles, the videoed barlines better represent the bar crest position. On average, the obtained distances between real and videoed bar positions Δr are 10–15 m, with the videoed barlines located shoreward. Changes in the bathymetric profile shape and the root-mean-squared wave height $H_{\rm rms}$ induce a variability of Δr of 16 m in La Barceloneta and 13 m in Bogatell. This apparent variability masks the real changes in bar position and should preferably be reduced before further analysis. As a highly significant correlation between Δr and $H_{\rm rms}$ is detected in the two beaches, the proposed reduction method consists of sampling at a specific range of $H_{\rm rms}$. This diminishes the variability by 10% to 14 m in La Barceloneta and 11 m in Bogatell. This paper confirms the suitability of using video systems for monitoring bars and terraces in the Barcelona beaches.**

Manuscript received June 5, 2009; revised October 29, 2009. Date of publication February 17, 2010; date of current version May 19, 2010. This work was supported by the Spanish Ministry of Science and Technology within the project SEDMET under Grant CTM2006-06919. The works of F. Ribas and E. Ojeda were supported by the Spanish government through the programs Juan de la Cierva and Formación del Profesorado Universitario, respectively. The work of T. D. Price was supported by the Netherlands Organization for Scientific Research under Contract 818.01.009.

F. Ribas was with the Institut de Ciències del Mar, Consejo Superior de Investigaciones Cientificas, Passeig Marítim de la Barceloneta, 08003 Barcelona, Spain. She is now with the Department of Applied Physics, Escola Politècnica Superior de Castelldefels, Universitat Politècnica de Catalunya, Campus del Baix Llobregat, 08860 Castelldefels, Spain, and also with the Unidad Asociada Universitat Politècnica de Catalunya, Consejo Superior de Investigaciones Cientificas Geología, Morfodinámica y Gestión Costera, 08034 Barcelona, Spain (e-mail: francesca.ribas@upc.edu).

E. Ojeda and J. Guillén are with the Institut de Ciències del Mar, Consejo Superior de Investigaciones Cientificas, 08003 Barcelona, Spain, and also with the Unidad Asociada Universitat Politècnica de Catalunya, Consejo Superior de Investigaciones Cientificas Geología, Morfodinámica y Gestión Costera, 08034 Barcelona, Spain (e-mail: eojeda@icm.csic.es; jorge@icm.cisc.es).

T. D. Price was with the Institut de Ciències del Mar, Consejo Superior de Investigaciones Cientificas, 08003 Barcelona, Spain. He is now with the Department of Physical Geography, Faculty of Geosciences, Institute for Marine and Atmospheric research Utrecht, Utrecht University, 3508 TA Utrecht, The Netherlands (e-mail: t.price@geo.uu.nl).

Color versions of one or more of the figures in this paper are available online at http://ieeexplore.ieee.org.

Digital Object Identifier 10.1109/TGRS.2009.2039576

Index Terms—**Geophysics, image analysis, remote sensing, sea coast, surface waves.**

I. Introduction

With the development of remote sensing techniques in the coastal zone during the last two decades, nearshore sciences have gained a new source of data with high temporal and spatial resolution [1], [2]. Many beaches worldwide are being monitored with video cameras (and occasionally X-band radar), technology that provides valuable information about the changes undergone by beach morphology and hydrodynamics over time. Obtaining these types of data sets is an essential first step in order to gain a deeper understanding of the physical mechanisms governing such complex environment.

Nearshore sandbars are shore-parallel accumulations of sand in natural beaches at depths of less than 10 m that have a fundamental importance in the study of surf-zone hydrodynamics, beach morphodynamics, and coastal protection. Understanding and predicting their dynamics is highly relevant, both in the cross-shore and in the alongshore directions (with the formation of crescents at scales of a few hundreds of meters, see [3]). The position and shape of sandbars does not respond immediately to a change in hydrodynamics, but there is a time lag between the change of wave conditions and the morphologic response. This time lag is a function of the intensity of the hydrodynamics and the volume of the sediment involved in the morphologic phenomenon [4].

The position of nearshore bars is visible in video images due to preferred breaking of waves at shallow areas. The foam created when waves break over a bar results in high-intensity areas in the time-averaged images. The cross-shore location of the *maximum video image intensity* $x_{\rm video}$ is often used as a measure for the *bar crest* or *minimum depth location* $x_{\rm crest}$ [5]. However, for each particular site, the relationship between these two quantities must be studied and established. The position $x_{\rm video}$ varies according to the parameters that control wave breaking, such as the wave height, the tidal level, and the shape of the underlying profile [6]. For example, the position $x_{\rm video}$ shifts immediately offshore when the wave height increases even with the actual bar crest remaining still. Some characteristics of the profile shape, such as the water depth above the bar or the bed slope at the seaward side of the bar crest, can also change the value of $x_{\rm video}$ for a given value of $x_{\rm crest}$. As a result of the varying hydrodynamics and local bathymetry on the one hand and the natural inertia of the bar position on the other hand, there is a time-varying offset

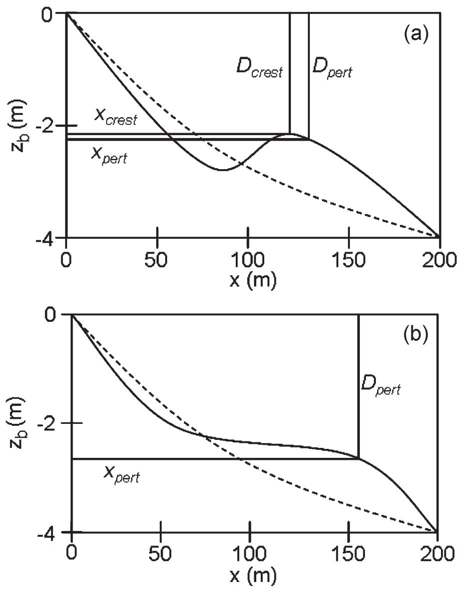

Fig. 1. Definitions of maximum perturbation location x_{pert} and the corresponding water depth D_{pert} and of bar crest location x_{crest} and the corresponding water depth D_{crest} for a (a) bar and a (b) terrace. The solid lines represent a measured profile and the dashed lines reproduce a featureless long-term averaged profile, identical in both panels.

between x_{video} and x_{crest}. The offset results in an apparent bar migration, unrelated to the actual bar migration, which must be evaluated and preferably reduced before performing further analyses of bar dynamics using video images.

A quantitative comparison of the actual bar crest position x_{crest} and the maximum intensity position in the images x_{video} has only been performed at a few sites. Lippmann and Holman [5] analyzed in detail the use of video images in Duck beach, USA, the first site where video cameras were installed starting up the Argus program [2]. They showed that x_{video} was indeed a good proxy for x_{crest}, with discrepancies of the order of 5%–10% and a maximum error of 35%. Although they expected x_{video} to be located seaward of x_{crest}, the contrary occurred in 42% of their observations. Plant and Holman [7] used another morphologic descriptor to quantify the bar position at Duck: the *position of maximum perturbation* of the actual profile with respect to a long-term averaged barless profile x_{pert} (Fig. 1). They also extended the study of [5] by quantifying the correlation between x_{video} and x_{pert} (Table I). The discrepancies between these two quantities were associated with changes in the underlying bathymetry and variations of the offshore wave height H_o. They found out that these discrepancies increased as bars moved seaward and as bar amplitude decreased. In addition, the discrepancies had a slight tendency to decrease as the offshore wave height increased.

Van Enckevort and Ruessink [6] performed a more detailed study at Egmond beach, The Netherlands, using both x_{crest} and x_{pert} to quantify bar position. They made a clear distinction between what they called Gaussian-shaped bars [those with a clear trough on the shoreward side, as shown in Fig. 1(a)], and terraced or platform-shaped bars [those with a subtle or even without a trough, see Fig. 1(b)]. In this paper, we will call them *bars* (or *barred profiles*) and *terraces* (or *terraced profiles*), respectively. Van Enckevort and Ruessink [6] showed that in the Egmond barred profiles x_{pert} corresponded well to the bar crest position x_{crest}, whereas these two quantities could differ by tens of meters in more terraced profiles. At their site, the videoed position x_{video} reflected the location of x_{pert} better than that of x_{crest}, the regression analysis giving better results in the former case (Table I). In general, x_{video} was located shoreward of x_{pert}, differing by a time varying distance $\Delta x = x_{\mathrm{video}} - x_{\mathrm{pert}}$ of the order of 10 m. This distance Δx displayed a linear relation with the offshore sea surface level η_o, Δx being closest to zero for low tide conditions and becoming more negative during high tide. No significant correlation between Δx and H_o was found. Moreover, [6] showed that the variability of Δx depended strongly on the actual bathymetric characteristics of the profiles, implying that their results could be significantly different at other sites. Ruessink *et al.* [8] analyzed the differences between x_{pert} and the bar position extracted from X-band radar images at the Egmond site. Their results were very similar to those obtained with video cameras (Table I).

Less detailed analyses have been performed at a small number of other sites, such as at Tairua beach, New Zealand [9]. Some of the conclusions for that site opposed those applying to Egmond beach. For instance, x_{video} was located seaward of x_{crest} in most of their observations (positive Δx, see Table I) and Δx was closer to zero during high tide. This confirmed that the variability of Δx can be strongly site dependent. Remarkably, the use of video images for detecting bar positions has only been assessed in sites located at open coasts with a significant tidal range of some 1.5 m, where the tidal oscillations explain most of the Δx variability.

Several mechanisms to remove the apparent bar migration due to the influence of hydrodynamics on x_{video} have been proposed in the literature. Kingston *et al.* [10] used an empirical neural network to model the cross-shore movement of the intensity maximum due to tides and waves. Then, they removed the resulting signal from the videoed bar position to obtain an accurate estimation of the real sandbar location in Egmond site. Van Enckevort and Ruessink [6] proposed simpler methods to remove the variability created by tidal oscillations. First, a single image per day sampled at low-tide was used, assuming that real changes in bar crest position occurred at time scales larger than one day, and this already reduced the standard deviation of Δx by 10%. Second, the slope m of the regression line of Δx versus the offshore tidal elevation η_o was obtained for the time period when the actual bar crest position was known (Table I). Subsequently, it was used to infer more accurately x_{pert} out of x_{video} in a more extensive data set (i.e., each videoed bar position was projected on a fixed tidal level). This further reduced the standard deviation of Δx by 30%, reaching a value of some 5.5 m. This correction method was also implemented by [11] and [12] to correct the x_{video} obtained for five different Argus sites. Ruessink *et al.* [8] applied a smoothing technique using an N-point symmetric Hanning window, which reduced the standard deviation Δx to nearly 3.2 m (Table I). However, they explained that this technique required the variation in η_o to be the dominant source of apparent Δx variability, so that it would fail in the case of tideless conditions.

Finally, considerable effort has been devoted to relate the cross-shore image intensity profiles $I(x)$ to the cross-shore

TABLE I
STATISTICAL RESULTS OF PREVIOUS STUDIES ON INFERRING NEARSHORE SANDBAR POSITIONS FROM VIDEO OR RADAR IMAGES

Reference *-video or radar-*	**Site (bar)**	**Tidal range (m)**	***N***	**Range of Δx (m)**	***Mean* Δx (m)**	***Std* Δx (m)**	**Regression analysis of x_{video} and x_{pert}**	**Regression analysis of η_o and Δx**	**Regression analysis of H_o and Δx**
Plant and Holman (1998) *-video-*	Duck (bar 2)	*1.0 - 1.3*	*60*	*(-55,20)*	*-13*	*21*	$r^2=0.78$ -	-	-
	Duck (bar 3)		*27*	*(-45,0)*	*-22*	*12*	$r^2=0.85$ -	-	-
van Enckevort and Ruessink (2001) *-video-*	Egmond (outer)	*1.3 - 1.8*	*363*	*(-35,-5)*	-	*9.5* 8.3^a $5.5^{a,b}$	$r^2=0.51$ $m=0.71$	$r^2=0.21$ $m=-5.9$	$\mathbf{r^2=0.02}$ $m=-4.7$
	Egmond (inner)		*781*	*(-30,5)*			$r^2=0.45$ $m=0.74$	$r^2=0.72$ $m=-14.6$	$\mathbf{r^2=0.01}$ $m=-2.8$
Ruessink et al. (2002) *-radar-*	Egmond (inner)	*1.4 - 2.1*	-	*(-40,15)*	*-7*	6.1^a $3.2^{a,b}$	$\mathbf{r^2=0.30}$ -	$r^2=0.83$ $m=-14.4$	-
Bryan & Swales (2003) *-video-*	Tairua	*~1.5*	*32*	*(-15,25)*	-	-	-	$r^2=0.85$ $m=-20.8$	$\mathbf{r^2=0.22}$ $m=-22.0$

Here, squared correlation coefficients, r^2, that are not significant at the 99% confidence level are shown in bold font, Δx is the distance between real and videoed bar positions, N is the number of distances available and m is the slope of the corresponding regression lines.

[a] Obtained after a selection of one daily low-tide image.

[b] Obtained after performing other η_o-corrections using different techniques (see the text for more details).

distribution of modeled physical quantities related to wave dissipation. Lippmann and Holman [5] concluded that the wave energy dissipation failed in reproducing $I(x)$. They pointed at the following source of error: With high waves, which get saturated across the whole surf zone, part of the surface foam remains floating after the wave pass and biases the image intensity shoreward. Later on, [6] showed that a better proxy for $I(x)$ is the energy dissipation of the surface roller, i.e., the aerated mass of water located on the shoreward face of a breaking wave. Recent works have focused on methods to minimize the impact of residual surface foam and link image intensity with roller dissipation derived from theoretical models [13]. The final aim of these elaborated transformations of the image intensity is to apply a depth inversion method and infer the beach bathymetry within the surf zone (see [14], and references therein). This technique can complement other depth inversion methods of bathymetric estimation based on measuring wave propagation characteristics (i.e., wave speed, wavenumber, etc.), which give reliable results in the shoaling domain but fail inside the surf zone (see [15] and references therein).

An Argus video system was installed atop a 142-m-high building close to the Olympic Marina of Barcelona city and started monitoring on October 20, 2001. An extensive analysis of the evolution of the shoreline during four years was performed by [16]. An important step in order to study the dynamics of the bar position with video images is to analyze the relationship between the maximum image intensity x_{video} and the real bar position. This is particularly crucial in Barcelona since it is a Mediterranean site, where wave and tide conditions differ significantly from the sites where similar methodological studies have been performed (Table I). Moreover, the bathymetric characteristics also differ from those of the previously studied beaches, the Barcelona ones displaying one single bar at most that often becomes a terrace.

The aim of this paper is to characterize the differences between the actual nearshore bar position measured in four bathymetric surveys from 2003 to 2006 and the corresponding maximum intensity obtained from video images at Barcelona city beaches. After presenting the study site and the available data in Section II, the methods for deriving the bar positions from *in situ* bathymetries and from video images will be detailed in Section III. The characteristics of the profile shapes in the available bathymetric surveys will be explained in Section IV. Section V will describe the differences between real and videoed bar positions, discussing separately the influence of the profile shapes and of the hydrodynamics. Section VI will discuss methods to reduce the variability of videoed bar position due to wave height variability and will compare this paper with the results at other sites. Finally, the overall conclusions will be listed in Section VII.

II. FIELD SITE AND DATA

La Barceloneta and Bogatell beaches are two of the man-made beaches of Barcelona city, located in the northeastern part of Spain (Fig. 2). Barcelona coast is part of the western Mediterranean Sea and shows microtidal conditions (tidal range < 0.20 m). Waves dominantly approach from northeastern, eastern, or southern directions. The annual average of the root-mean-squared wave height H_{rms} is 0.5 m, but during storms, the maximum H_{rms} can be up to 3 m. Wave heights are characterized by a cyclic behavior: Stormy periods occur from October to April, whereas periods with low storm activity occur from May to September. The most important storms approach from the east, and they are often associated with the cyclonic activity in the western Mediterranean, with a typical duration of a few days [16].

La Barceloneta has a length of approximately 1100 m and is orientated 20° from the north, whereas Bogatell has a length

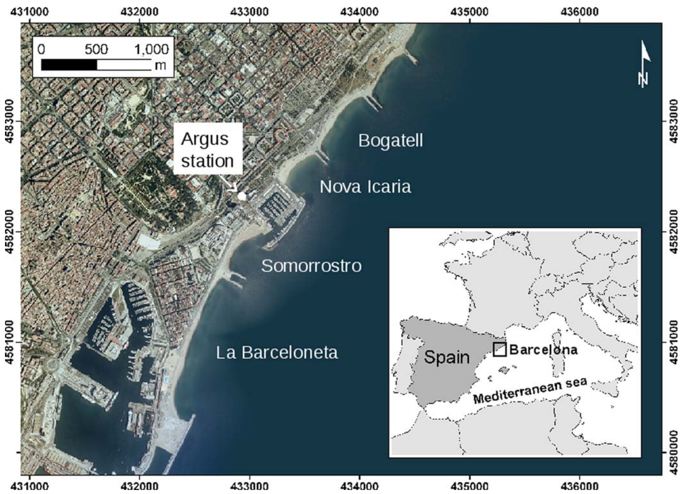

Fig. 2. Location of the Argus station and the closest beaches of Barcelona city, from north to south: Bogatell, Nova Icaria, Somorrostro, and La Barceloneta. The coordinates are given in UTM.

of 600 m and is orientated 38° from the north. Both beaches are confined between two shore-normal groins, the southern groin of La Barceloneta being L-shaped (Fig. 2). The sediment sizes (D_{50}) on these beaches range between 0.43 mm (at some 5-m depth) and 1.5 mm (on the dry beach). Barcelona beaches are often affected by small-scale human interventions such as sand redistribution after storms. Moreover, major nourishment projects took place in July 2002 [17] and in March and June 2006.

The Argus station of Barcelona city consists of five full-color cameras, which offer a 180° view of the four beaches surrounding the marina (Fig. 2). Every daylight hour, during a 10-min period, the cameras make 600 individual *snap-shot* images per camera. The *timex* images are obtained from the average of these 600 individual snap-shot images, and result in a filter of the high-frequency changes in wave breaking patterns. Finally, the timex images from the five cameras are rectified and merged to obtain a planview of the study area [1]. Stripes of high intensity that correspond to shallower zones can be distinguished in such planviews, as shown in the examples of Fig. 3. After transforming the image coordinates to real world coordinates, the cross-shore and alongshore coordinates increase seaward and northward, respectively, and their origin is the location of the video cameras. The obtained pixel resolution ranges from 1 to 1.5 m in the cross-shore direction and from 1 to 10–20 m in the alongshore direction. The worst alongshore resolution is obtained at the far end of Bogatell (10 m at $y = +1100$ m) and La Barceloneta (20 m at $y = -2100$ m). The time period studied in the present contribution is from October 20, 2001 (first day with video images) to November 15, 2006, when the construction of a new shore-parallel groin in La Barceloneta beach changed completely its morphodynamic behavior. The video system worked continuously during the entire five years.

Data from a directional wave buoy located in front of Barcelona harbor, at 69-m depth, were available since March 2004 (Cost-Barcelona buoy). In earlier periods, wave conditions were obtained from the WANA model data set (node WANA2066051), computed by the Spanish National Institute of Meteorology using the HIRLAM and WAM numerical models. The most energetic winters during the study period occurred in 2001–2002 and in 2003–2004, with peaks of $H_{\rm rms}$ higher than 3 m (Fig. 4). The sea surface level η_o was measured in a buoy located inside the harbor of Barcelona. The mean η_o at this point is 0.26 m, measured with respect to the Spanish vertical datum of reference. Higher sea levels are found during low pressure periods in autumn. The two highest η_o during the study period (0.8–0.9 m) were reached in November 2001 and October 2003, respectively (Fig. 4).

Four nearshore bathymetries were measured during the study period: October 4, 2003, November 5, 2003, October 26, 2005, and November 10, 2006 (Fig. 3). Bottom bathymetry was measured from approximately 0.5- to 15-m water depth along cross-shore profiles at some 50-m of alongshore spacing, using echo sounding from a boat and a dGPS system. The topography of the dry beach was measured with a dGPS system, and it was added to the bathymetric profiles. The coordinate system used was the same as in the planviews and the sea surface level. The number of measured profiles depended on the surveys, ranging from 12 to 22 in La Barceloneta and from 5 to 10 in Bogatell. In total, 55 profiles were available for La Barceloneta and 26 for Bogatell. The profiles of both beaches exhibited a single nearshore bar at most (Fig. 3). Since Nova Icaria and Somorrostro were constant-sloping featureless beaches, they were not included in this paper.

III. METHODS FOR EXTRACTING BAR POSITION

A. *Deriving Bar Characteristics From Cross-Shore Profiles*

As introduced in Section I, there are several parameters that can describe the cross-shore characteristics of a barred profile. In the majority of the videoed sites described in the literature, the bars consist of a clear trough and a seaward located shallower bar crest (e.g., [5] and [9]). In these cases, the bar crest position $x_{\rm crest}$ provides a good descriptor for characterizing the bar location. At the sites where the bars are not Gaussian-shaped but more platform or terraced shaped, the location of the bar may be characterized by the position of maximum difference between the actual profile and the long-term averaged featureless profile, known as the position of maximum perturbation $x_{\rm pert}$ [7]. Since no long-term bathymetric measurements were available for Barcelona beaches, the bar location in the case of terraced profiles was characterized by *the position of the terrace edge* or *slope break*, $x_{\rm edge}$, defined as the location of maximum slope change. This location is very close to the position of maximum perturbation $x_{\rm pert}$ [5]. In this paper, $x_{\rm edge}$ will always be referred to as the terrace edge, and it will also be calculated in the case of barred profiles (Fig. 5).

Fig. 3 shows examples of the different profile shapes of the two Barcelona beaches during the study period. In general, the profiles at La Barceloneta presented a more developed bar in contrast to the profiles at Bogatell, which exhibited a more terraced shape often without a trough. The bathymetries were both alongshore variable. In the north of La Barceloneta, the profiles were often featureless, particularly in 2005 and 2006

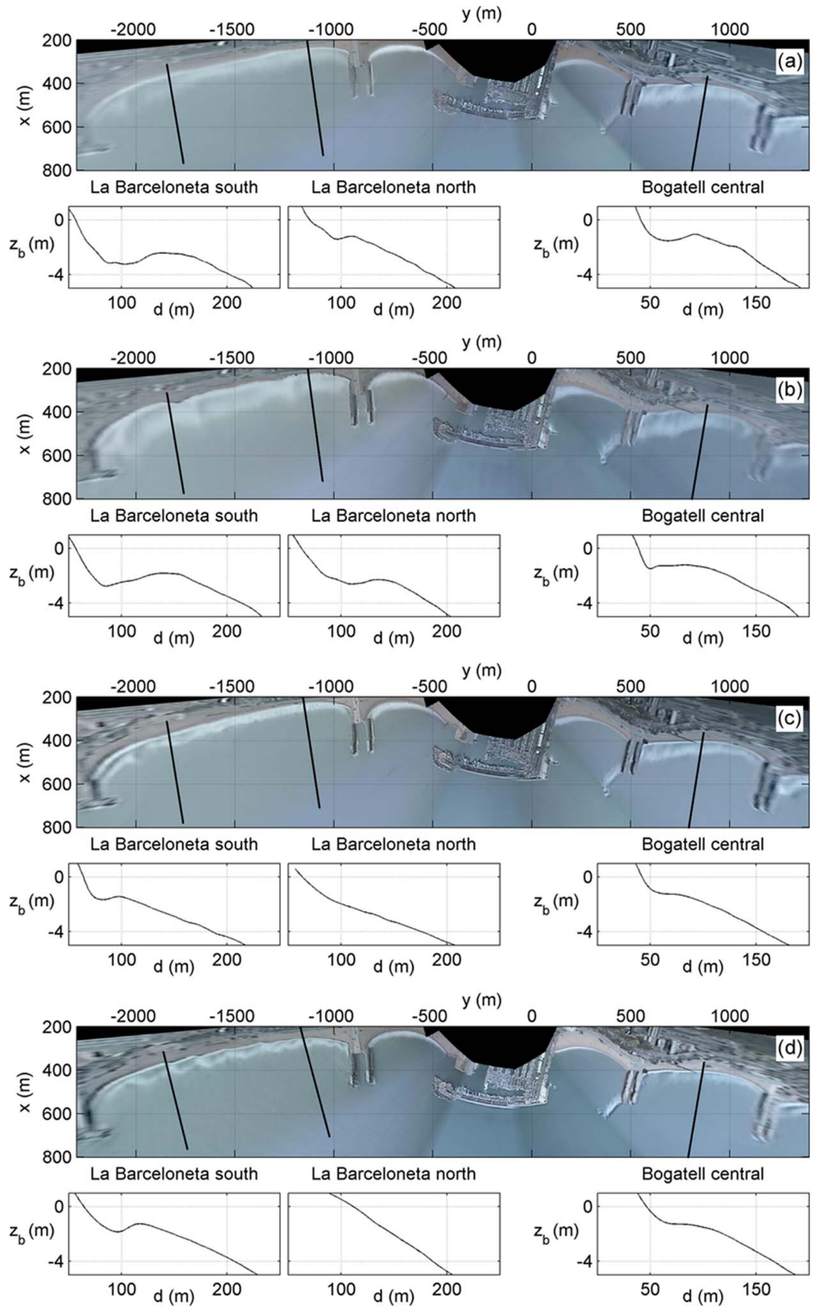

Fig. 3. Examples of planviews and bathymetric transects along with the corresponding profiles of the four bathymetries measured on (a) October 4, 2003 (image from October 15, 2003 at 8 h), (b) November 5, 2003 (image from November 8, 2003 at 14 h), (c) October 26, 2005 (image from November 23, 2005 at 13 h), and (d) November 10, 2006 (image from November 4, 2006 at 15 h). In the profiles, z_b is the bed level and d is the distance from a reference line, measured along the corresponding transect.

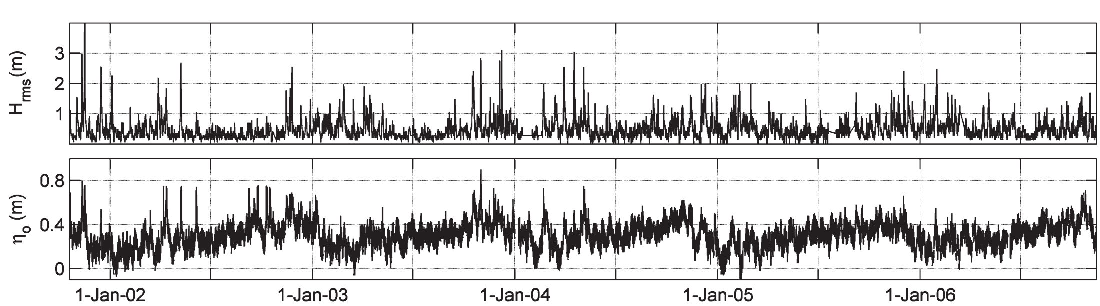

Fig. 4. (Upper panel) Root-mean-squared wave height and (lower panel) sea surface level measured during the study period.

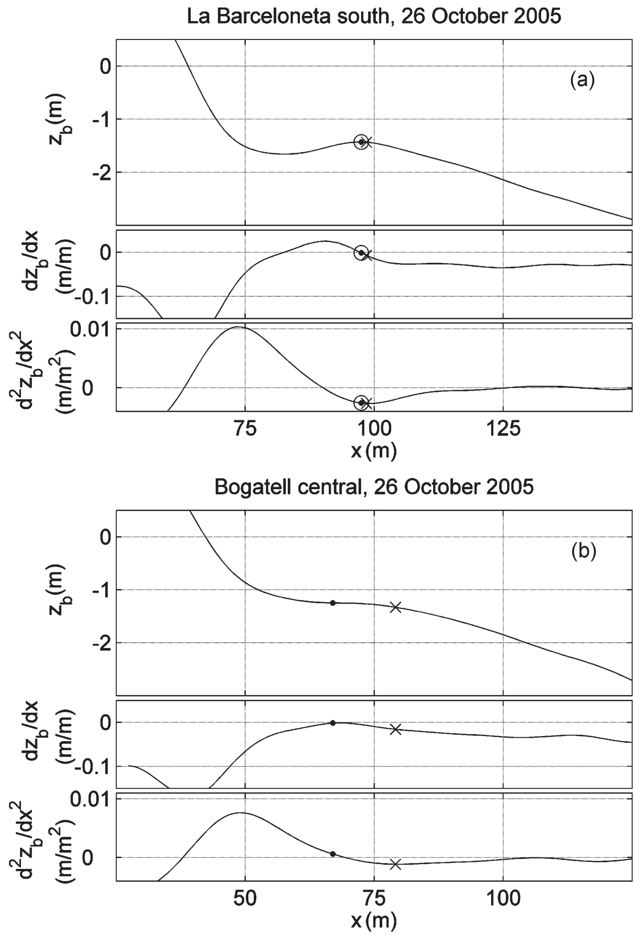

Fig. 5. Quantitative determination of the morphologic descriptors in (a) La Barceloneta southern cross-shore profile and in (b) Bogatell central profile from the bathymetry on October 26, 2005 (see Fig. 3). The panels display, from top to bottom, the bed level, z_b, the first derivative of the bed level, dz_b/dx, which equals minus the slope, and the second derivative of the bed level, d^2z_b/dx^2, which equals minus the slope change. The bar crest is indicated by a circle sign ($\circ$), the terrace edge is indicated by a cross sign ($\times$) and the slope at the bar/terrace is taken at the dot sign ($\bullet$).

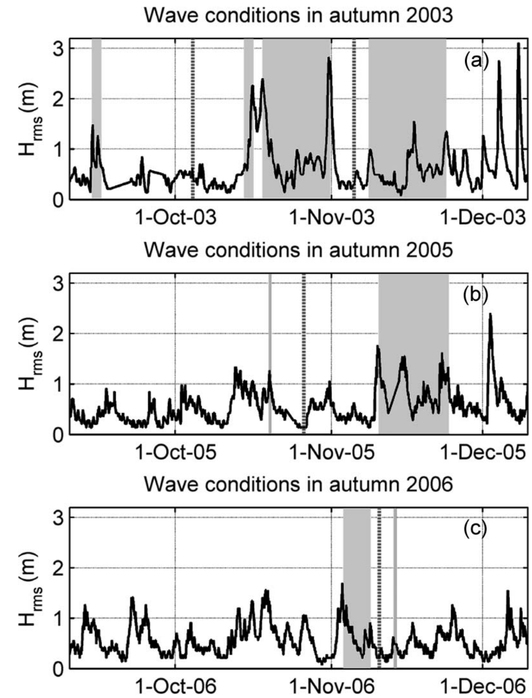

Fig. 6. Time series of H_{rms} during (upper panel) autumn 2003, (middle panel) autumn 2005, and (lower panel) autumn 2006. Vertical dashed dark gray lines indicate the date of bathymetric surveys. Gray rectangles indicate the period when barlines were sampled for each bathymetry.

[Fig. 3(c) and (d)], and they became clearly barred toward the center and the south. In both beaches, the bar/terrace was obliquely oriented, with the southern part being located at larger water depths.

Before starting the quantitative extraction of the bar position from the bathymetric profiles, each profile was qualitatively classified as featureless, terraced, or barred from visual observation. Then, the position and characteristics of the bar crest and the terrace edge of all the cross-shore profiles were determined. In the case of barred profiles, both locations were tracked for a matter of comparison, whereas only the terrace edge was determined for terraced profiles (since they have no points of local minimum depth). As the Barcelona beaches have a certain curvature, both the cross-shore and the alongshore coordinates were determined $\boldsymbol{r_{edge}} = (x_{\mathrm{edge}}, y_{\mathrm{edge}})$ and $\boldsymbol{r_{crest}} = (x_{\mathrm{crest}}, y_{\mathrm{crest}})$. The position $\boldsymbol{r_{edge}}$ and the corresponding parameters were also extracted from the featureless profiles for comparison.

Fig. 5(a) shows an example of the determination of the two locations for a clearly barred profile in La Barceloneta. The bar crest occurs where the first derivative of the bed level dz_b/dx is zero downcrossing [circle sign on Fig. 5(a)]. Seaward of the bar crest, dz_b/dx decreases rapidly to a value of -0.03. The terrace edge, visible as a minimum of the second derivative of the bed level, d^2z_b/dx^2 [cross sign on Fig. 5(a)], lies slightly seaward of the bar crest. Seaward of the terrace edge d^2z_b/dx^2 increases up to a value around zero and indicates that the slope remains constant.

Fig. 5(b) shows an example of the quantification of the terrace edge location for a terraced profile in Bogatell. The terraced nature of the profile is illustrated by the first derivative of the bed level, where the terrace appears as a section with a relatively small slope (dz_b/dx near zero), followed by a decrease of dz_b/dx in the offshore direction. Further offshore the profile reaches again a relatively constant value of dz_b/dx of some -0.03. The decrease in dz_b/dx indicates the area of the terrace edge, and its exact location is defined by the minimum in d^2z_b/dx^2 [cross sign in Fig. 5(b)]. The slope at the terrace, calculated as the slope closest to zero shoreward of the terrace edge (dot signs in Fig. 5), was also determined for both terraces and bars (in the latter case, its theoretical value is zero).

B. Deriving Bar Positions From Video Images

The planview timex images, obtained after averaging, rectifying, and merging the five oblique images from the video cameras, were first visualized in order to select candidate images with clear barlines. The frequent occurrence of $H_{\mathrm{rms}} < 0.5$ m precluded barline detection due to lack of breaking over the bar (the threshold value being larger if the bar was located deeper). On the other extreme, in case of $H_{\mathrm{rms}} > 3$ m, a wide breaking zone occupied the whole nearshore making barline detection

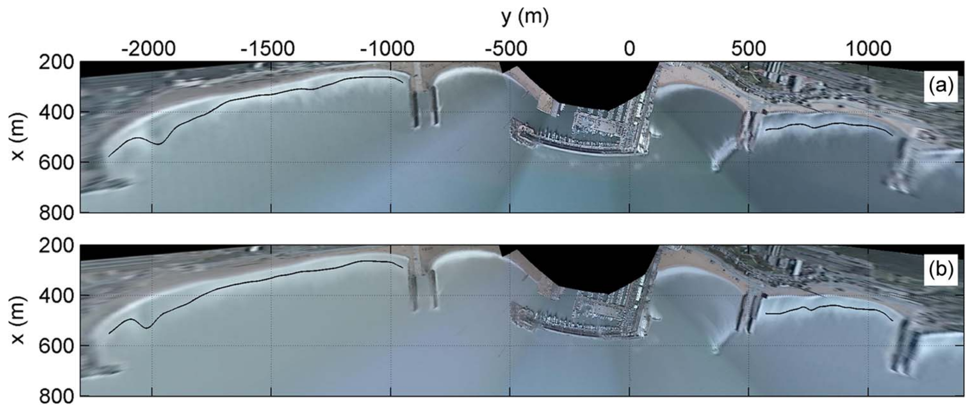

Fig. 7. Planview images on (a) September 15, 2003 at 13 h and on (b) October 15, 2003 at 12 h, with the corresponding barlines sampled for the bathymetric survey performed on October 4, 2003. The $H_{\rm rms}$ was 1.1 m in (a) and 1.0 m in (b).

unclear (the threshold being again variable). The maximum intensity lines $\boldsymbol{r_{video}} = (x_{\rm video}, y_{\rm video})$ were extracted from the candidate planview images by an automated alongshore tracking of the intensity maxima across each bar, as detailed in [3]. These lines are referred to as barlines and represent the planview bar morphology obtained from the video images. To reduce the alongshore noise of the barlines, they were low-pass filtered using a Hanning window. The groins at either side of the beaches prevented wave breaking at certain sections of the bar (particularly in the case of oblique angles of wave incidence) and sometimes caused the detection of inaccurate barlines near them. The barlines were thereby revised and incorrect sections were manually removed.

Mainly due to the long periods of low energetic conditions and the tideless nature of our site, the interval between subsequent video observations of barlines was highly irregular. As previously mentioned, candidate images for sampling barlines were only available if wave conditions were adequate during daylight hours. Bearing also in mind that large waves induce bathymetric changes, $\boldsymbol{r_{video}}$ was extracted from the images for comparison with the real bar position the first two days with candidate images before and after the date of the bathymetric survey. In total, some 10–20 barlines were sampled for each bathymetry, those nearest in time to the survey date. Barlines were never sampled more than one month before or after the survey. Fig. 6 shows the $H_{\rm rms}$ measured at the time of the bathymetric surveys, with an indication of the periods where videoed barlines were sampled for each bathymetry. Sometimes barlines were sampled in different moments for each beach. For instance, in 2003, the bar was situated at larger water depths in La Barceloneta than in Bogatell [Fig. 3(a) and (b)], requiring larger wave heights for barline extraction. Given the relatively long time span between certain bathymetric surveys and the corresponding image barline sampling, the planviews and the barlines sampled (at similar wave heights) prior and after each survey were checked to verify that they showed no significant change in their configuration (see Fig. 7 as an example for the survey on October 4, 2003). The wave conditions are commonly calm during the periods when barlines cannot be sampled, in which case no significant bathymetric changes are induced either.

In total, 55 barlines were sampled for La Barceloneta and 57 barlines were sampled for Bogatell. These $\boldsymbol{r_{video}}$ were used for comparison with the two locations that can characterize the actual bar position $\boldsymbol{r_{crest}}$ and the $\boldsymbol{r_{edge}}$ determined in Section III-A. With this aim, the distances between them were calculated $\Delta r_{\rm crest}$ and $\Delta r_{\rm edge}$. Given the fact that both beaches have a certain curvature (Fig. 3), the distance was computed for each cross-shore bathymetric transect as the minimum distance between each bathymetric crest/edge position and the corresponding complete barline

$$\begin{aligned}\Delta r_{\rm crest} &= {\rm sign}\ \min\left(\sqrt{(x_{\rm video}-x_{\rm crest})^2+(y_{\rm video}-y_{\rm crest})^2}\right)\\ \Delta r_{\rm edge} &= {\rm sign}\ \min\left(\sqrt{(x_{\rm video}-x_{\rm edge})^2+(y_{\rm video}-y_{\rm edge})^2}\right).\end{aligned} \tag{1}$$

The sign is equal to $+1$ if the morphologic descriptor is located shoreward of the barline and equal to -1 if it is located seaward. For each cross-shore transect of all the bathymetries, as many distances as available barlines were computed.

IV. Characteristics of the Available Profiles

In addition to the qualitative visual classification described in Section III-A, profile characteristics were analyzed in order to find out quantitative criteria to distinguish between barred, terraced, or featureless profiles. In this way, the presence of a barred or terraced profile could be validated before comparing the real bar locations and the videoed locations (as waves also break on featureless profiles). A barred profile can be distinguished from a terraced profile by the presence of a local minimum depth, corresponding to the bar crest. A terraced profile differs from a featureless profile due to the successive presence (following the offshore direction) of a relatively small constant slope, a clear slope break (or terrace edge) and a larger constant slope (Fig. 5). In order to validate the presence of terraced profiles, the value of the terrace slope and the values of the maximum slope change and the water depth at the terrace edge were compared for all terraced and featureless profiles. The values of these profile parameters, which affect the wave

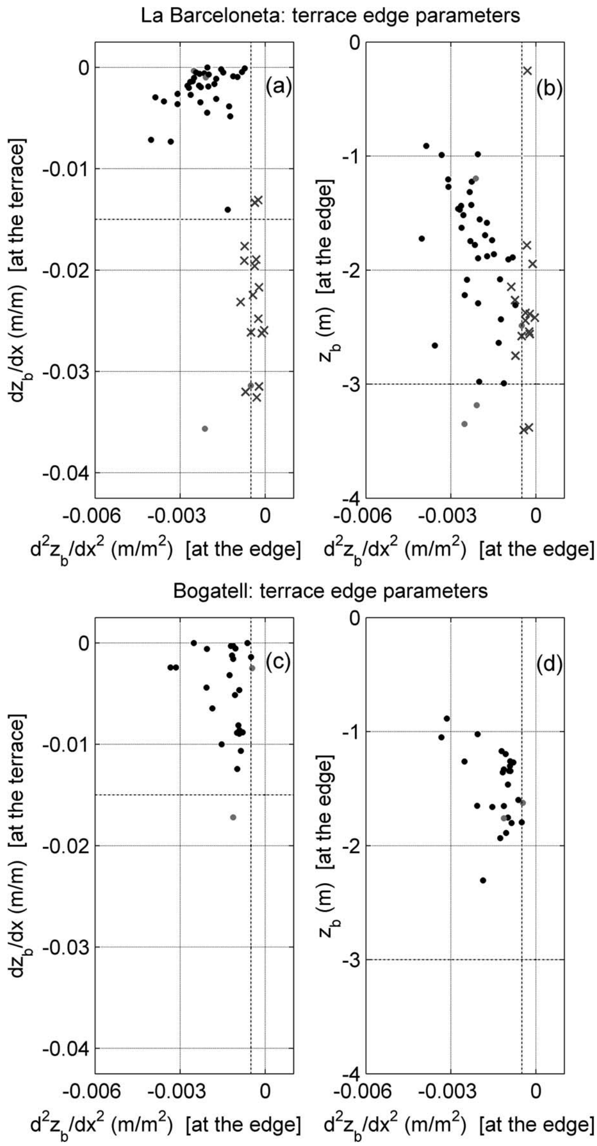

Fig. 8. Characteristics of the terrace edges in La Barceloneta [terrace slope in (a) and bed level at the terrace edge in (b) versus maximum slope change] and in Bogatell [terrace slope in (c) and bed level at the terrace edge in (d) versus maximum slope change] for all the terraced and featureless cross-shore profiles. The clear and shallow terraced cross-shore profiles are marked with a black dot, the unclearly or too deeply terraced cross-shore profiles with a gray dot and the visually observed featureless cross-shore profiles with a gray cross. The dot-dashed lines indicate the distinguishing criteria of Table II.

breaking process, were also kept to study their influence on the distances Δr.

Fig. 8(a) and (b) shows the characteristics of the terrace edges for all the profiles of the four bathymetries of La Barceloneta. In panel (a), clearly terraced profiles (black dots) form a cluster of points with a small terrace slope (dz_b/dx close to zero) and a distinct slope change (a large negative value of d^2z_b/dx^2). On the other hand, the featureless profiles (gray crosses) exhibit larger terrace slopes (large negative values of dz_b/dx) and indistinct slope breaks (d^2z_b/dx^2 close to zero). The majority of these profiles, which are used as examples of invalid profiles, were measured at the north of La Barceloneta on October 26, 2005 [Fig. 3(c)]. Based on these two clusters, limiting values for the terrace slope and the slope break were

TABLE II
DISTINGUISHING CRITERIA FOR CLEAR AND SHALLOW TERRACED PROFILES

d^2z_b/dx^2 at the terrace edge (m/m^2)	< *-0.0005*
dz_b/dx at the terrace (m/m)	> *-0.015*
z_b at the terrace edge or bar crest (m)	> *-3.0*

TABLE III
QUANTITATIVE CLASSIFICATION OF ALL THE AVAILABLE PROFILES

	All the profiles	**La Barceloneta profiles**	**Bogatell profiles**
Shallow bars	53%	58%	42%
Shallow terraces	20%	5%	50%
Unclear terraces	4%	2%	8%
Deep bars/terraces	2%	4%	0%
Featureless profiles	21%	31%	0%

estimated in order to differentiate quantitatively between the clearly terraced profiles and the unclearly terraced or featureless profiles (Table II and dot-dashed lines in Fig. 8). Moreover, Fig. 8(b) shows that indistinct slope breaks are located at larger water depths, implying the requirement for a maximum water depth at the slope break (indeed, most of the waves propagate without breaking above too deep bars/terraces). Overall, the distinguishing criteria resulted in only three profiles of La Barceloneta (measured on November 5, 2003) to be classified as *unclear* or *deep terraces* (gray dots).

Fig. 8(c) and (d) shows the profile characteristics at Bogatell. All the profiles were visually classified as terraced profiles, and only two of them did not verify the criteria for the terrace slope and the maximum slope break determined for the profiles at La Barceloneta. The terrace edges of the Bogatell profiles were located at smaller water depths than in La Barceloneta and none of them were classified as too deep.

Following the criteria of Table II, all the available profiles were classified quantitatively as *shallow bars*, *shallow terraces*, *unclear terraces, deep bars/terraces*, or *featureless profiles*, the latter being detected visually. Table III shows the relative occurrence of each type that was found in the four bathymetries, detailing the percentages at the two beaches to enlighten their distinctive bathymetric properties. Only 53% of the profiles in Barcelona beaches exhibited a shallow bar and 20% of the profiles exhibited a shallow, clear terrace. More than 25% of the available profiles were either featureless or with unclear or too deeply located bars/terraces. There was a more significant presence of bars in La Barceloneta and a dominance of terraces in Bogatell. The clear and shallow terraces and bars are those considered to be *valid profiles* in this paper. In total, 468 distances were obtained for the valid profiles in La Barceloneta using the terrace edge location and 415 using bar crests. In Bogatell, 326 distances were obtained using terrace edges and only 152 using bar crests.

TABLE IV
STATISTICAL RESULTS OF THE DISTANCES FOR THE TWO BEACHES AND THE TWO DESCRIPTORS

Statistical descriptor	**La Barceloneta (using r_{edge})**	**La Barceloneta (using r_{crest})**	**Bogatell (using r_{edge})**	**Bogatell (using r_{crest})**
Number of values, N	*468*	*415*	*326*	*152*
Mean (Δr) (m)	*-13.0*	*-8.3*	*-15.2*	*-6.9*
Std (Δr) (m)	*17.6*	*15.6*	*13.0*	*10.0*
Mean ($\lvert\Delta r\rvert$) (m)	*17.9*	*14.8*	*16.7*	*10.3*

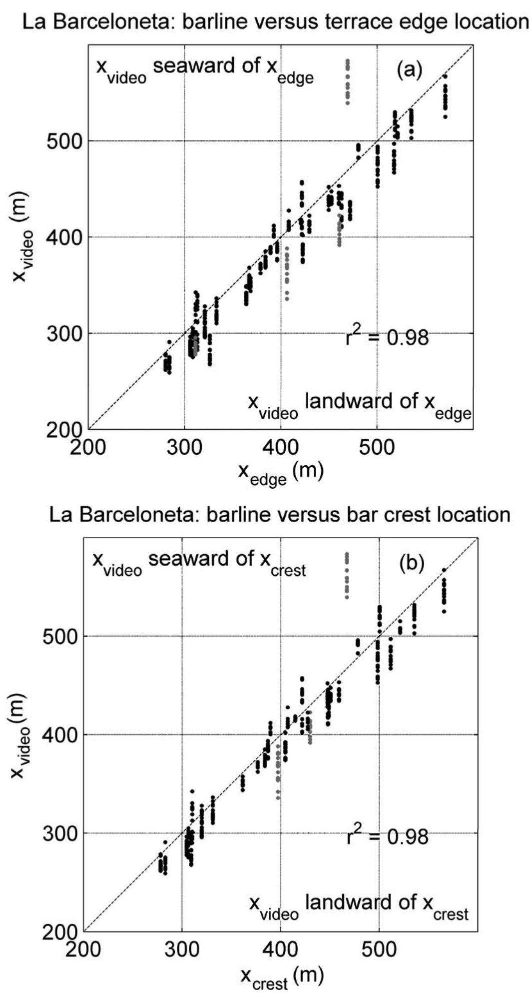

Fig. 9. Plots of (a) x_{video} versus x_{edge} and of (b) x_{video} versus x_{crest} at La Barceloneta for both the (black dots) valid profiles and the (gray dots) deeply or unclearly barred/terraced profiles. The drawn dashed line in each plot is the line of equality.

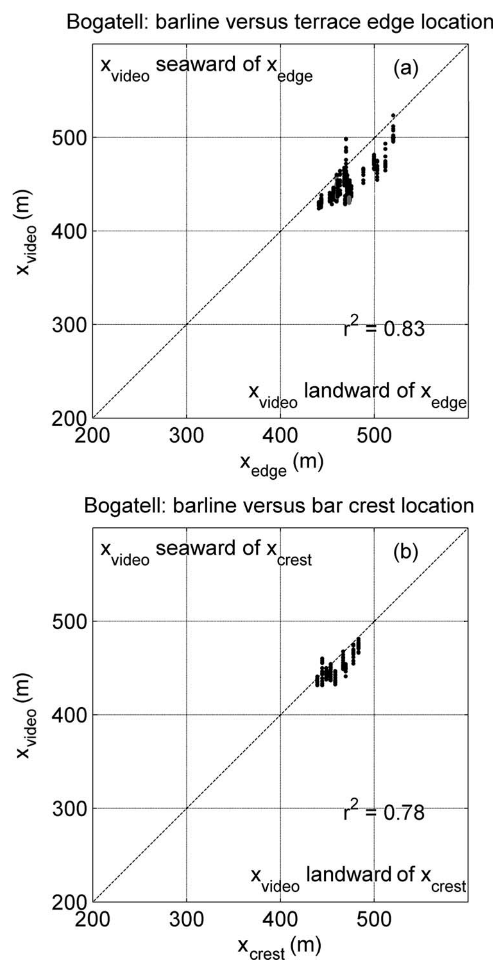

Fig. 10. Plots of (a) x_{video} versus x_{edge} and of (b) x_{video} versus x_{crest} at Bogatell for both the (black dots) valid profiles and the (gray dots) deeply or unclearly barred/terraced profiles. The drawn dashed line in each plot is the line of equality.

V. CHARACTERISTICS OF THE DISTANCES BETWEEN REAL AND VIDEOED BAR POSITIONS

The distances Δr obtained for the valid profiles were of the order of 10 m, showing minimum values of some -50 m and maximum values of some $+25$ m. Table IV displays the statistical descriptors of Δr using the two morphologic positions, $\boldsymbol{r_{edge}}$ and $\boldsymbol{r_{crest}}$ (for comparison). The results are given separately for the two beaches due to the differences in their bathymetric characteristics. The negative values for the mean distances, $mean(\Delta r)$, show that the barline positions, $\boldsymbol{r_{video}}$, were located shoreward of the real morphologic positions on average. The videoed barlines in Barcelona reflected the location of the bar crest better than that of the terrace edge, indicated by the smaller values for both $mean(\Delta r_{\mathrm{crest}})$ and $std(\Delta r_{\mathrm{crest}})$. The absolute mean distances were also larger for the terrace edge location $\boldsymbol{r_{edge}}$ than for the bar crest position $\boldsymbol{r_{crest}}$. The standard deviations of the distances $std(\Delta r)$ were larger in La Barceloneta than in Bogatell. A significantly smaller amount of values for $\Delta r_{\mathrm{crest}}$ were available in Bogatell, where bar presence was less frequent (Table III).

TABLE V
RESULTS OF THE REGRESSION ANALYSIS OF THE STUDY

La Barceloneta beach					Bogatell beach				
X	*Y*	*m*	*b (m)*	r^2	*X*	*Y*	*m*	*b (m)*	r^2
x_{edge}	x_{video}	0.97	-4.9	0.98	x_{edge}	x_{video}	0.75	98	0.83
x_{crest}	x_{video}	1.00	-10.4	0.98	x_{crest}	x_{video}	0.74	112	0.78
$-z_{b,edge}$	Δr_{edge}	-11.5	8.16	-0.35	$-z_{b,edge}$	Δr_{edge}	-5.70	-6.91	**-0.15**
$-z_{b,crest}$	Δr_{crest}	-4.89	0.794	**-0.16**	$-z_{b,crest}$	Δr_{crest}	7.47	-16.6	**0.23**
H_{rms}	Δr_{edge}	8.76	-24.5	0.31	H_{rms}	Δr_{edge}	5.35	-21.9	0.24
H_{rms}	Δr_{crest}	8.60	-19.5	0.34	H_{rms}	Δr_{crest}	4.11	-11.4	**0.23**
H_{rms}/D_{edge}	Δr_{edge}	28.8	-30.0	0.47	H_{rms}/D_{edge}	Δr_{edge}	15.8	-25.4	0.31
H_{rms}/D_{crest}	Δr_{crest}	24.7	-22.4	0.41	H_{rms}/D_{crest}	Δr_{crest}	5.82	-10.5	**0.15**
η_o	Δr_{edge}	-9.53	-8.59	**-0.06**	η_o	Δr_{edge}	-7.35	-11.5	**-0.07**
η_o	Δr_{crest}	-9.07	-4.08	**-0.07**	η_o	Δr_{crest}	-0.53	-6.48	**-0.01**

Here, $Y=mX+b$, the water depth, $D=\eta_o-z_b$, is computed using the free surface level, and squared correlation coefficients, r^2, that are not significant at the 99% confidence level are shown in bold font.

It is known that Δr can vary temporally and spatially due to changes of $H_{\rm rms}$, the sea surface level, η_o, and the local shape of the bathymetric profiles [6]. The alongshore variation of the cross-shore profiles (particularly when changing from La Barceloneta to Bogatell) were used to study qualitatively the bathymetric effects on Δr. The temporal variation of the offshore wave height and the sea surface level was used to study the hydrodynamic effects on Δr.

A. Bathymetric Effects on the Distances

As shown in Section IV, the cross-shore profiles of La Barceloneta and Bogatell varied alongshore, resulting in different responses of the videoed barlines. A comparison between videoed and real bar cross-shore positions is shown in Figs. 9 and 10. The bar obliquity in both beaches allows the distinction of different cross-shore profiles to be made. In general, the two morphologic descriptors $x_{\rm edge}$ and $x_{\rm crest}$ were highly correlated with $x_{\rm video}$ in both beaches (Table V).

In La Barceloneta beach, the majority of $x_{\rm video}$ lied landward of $x_{\rm edge}$, the points being located below the line of equality [Fig. 9(a)]. The profiles with deep or unclear bars/terraces, plotted as gray dots, showed the largest deviations of $x_{\rm video}$. A large water depth over the bars/terraces inhibits the morphology to control wave breaking, causing waves to break on the slope onshore of the bar. Unclear slope breaks do not provide defined locations which control wave breaking, allowing the barline to move freely across the cross-shore profile, depending on the slope and the change in wave height. When comparing the two panels of Fig. 9, the proximity of $x_{\rm video}$ to $x_{\rm crest}$ is again apparent, the slope of the corresponding regression line being $m = 1$ (Table V). In Bogatell beach, nearly all the values of $x_{\rm video}$ lied landward of $x_{\rm edge}$ or $x_{\rm crest}$ (Fig. 10). Given the smaller length and different bar orientation found in Bogatell beach, a minor range of cross-shore locations x was obtained, affecting the regression analysis.

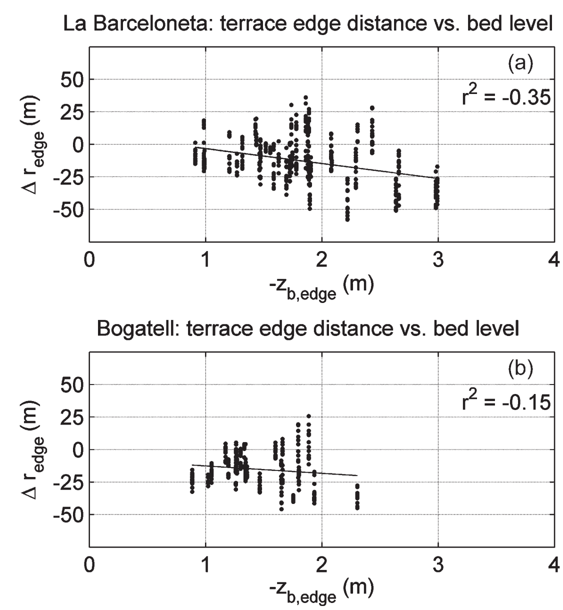

Fig. 11. Variation of $\Delta r_{\rm edge}$ with minus the bed level at the terrace edge $-z_{b,edge}$ for the valid profiles at La Barceloneta beach (a) and at Bogatell beach (b). Positive (negative) values of Δr indicate that the videoed bar position lies seaward (landward) of the real bar position.

The bed level at the terrace edge or bar crest is an important property to understand the cross-shore distribution of wave breaking and the corresponding position r_{video}. As an example, Fig. 11 shows the values of $\Delta r_{\rm edge}$ in La Barceloneta and Bogatell as a function of minus the bed level over the terrace edge $-z_{b,edge}$. In general, the variability of $\Delta r_{\rm edge}$

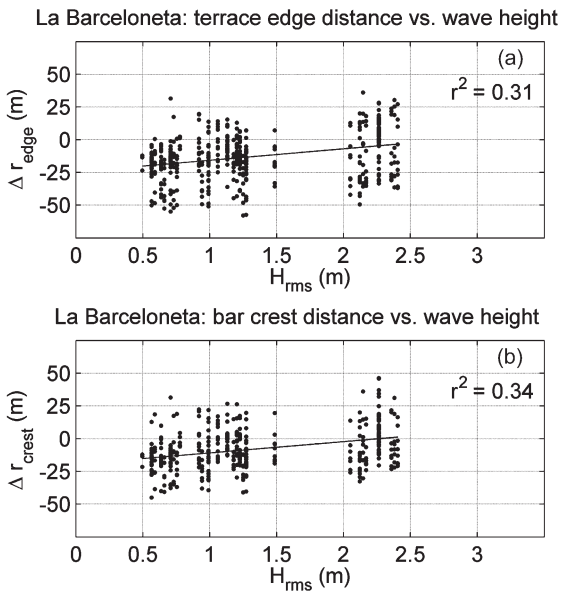

Fig. 12. Variation of Δr with the offshore wave height H_{rms} using the (a) terrace edge location and using the (b) bar crest location at La Barceloneta beach, for the valid profiles. Positive (negative) values of Δr indicate that the videoed bar position lies seaward (landward) of the real bar position.

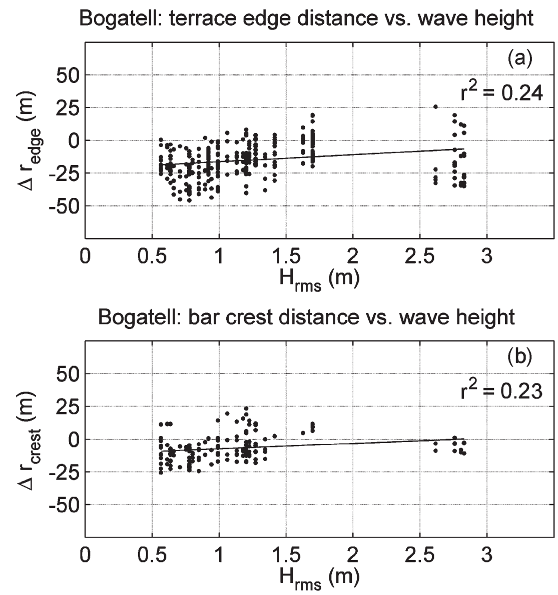

Fig. 13. Variation of Δr with the offshore wave height H_{rms} using the (a) terrace edge location and using the (b) bar crest location at Bogatell beach, for the valid profiles. Positive (negative) values of Δr indicate that the videoed bar position lies seaward (landward) of the real bar position.

increased if the terrace edge was located deeper. Moreover, in La Barceloneta, Δr_{edge} became more negative ($\boldsymbol{r_{video}}$ landward of $\boldsymbol{r_{edge}}$) for deeply located terrace edges [Fig. 11(a)], the corresponding squared correlation coefficient r^2 being significant at the 99% confidence level (Table V). A larger amount of waves can propagate without breaking over a deeply located bar/terrace, $\boldsymbol{r_{video}}$ becoming more variable and shoreward located on average. In Bogatell, however, this effect was less apparent because the bar/terrace was always located in shallow regions [Fig. 11(b)].

B. Hydrodynamic Effects on the Distances

Figs. 12 and 13 show the values of Δr as a function of the offshore H_{rms} for La Barceloneta and Bogatell, respectively. The H_{rms} corresponding to the images used for barline acquisition varied between 0.5 and 2.4 m for the La Barceloneta barlines and between 0.6 and 2.8 m for the Bogatell barlines. For both beaches, Δr was more negative for small H_{rms} values and increased approximately linearly with increasing wave height. This was the expected pattern, the waves with larger height breaking further seaward than those with smaller height. The characteristics of the corresponding regression lines are shown in Table V. In La Barceloneta, the line of the best linear fit was very similar for both location descriptors. All the squared correlation coefficients r^2 were significant at the 99% confidence level, except for the one of the correlation between Δr_{edge} and H_{rms} in Bogatell [Fig. 13(b)], which was only significant at the 95% confidence level (partly due to the smaller amount of distances available).

Subsequently, the relationship between the distances Δr and the sea surface level η_o was investigated. The η_o corresponding to the images used for barline acquisition varied between 0.2 and 0.7 m for the La Barceloneta barlines and between 0.3 and 0.85 m for the Bogatell barlines. Fig. 14 shows the

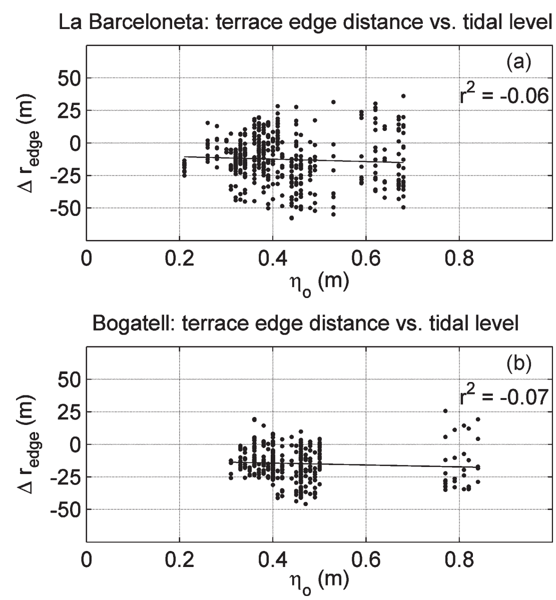

Fig. 14. Variation of Δr_{edge} with the sea surface level η_o, at (a) La Barceloneta beach and at (b) Bogatell beach, for the valid profiles. Positive (negative) values of Δr indicate that the videoed bar position lies seaward (landward) of the real bar position.

corresponding plots for Δr_{edge} in both beaches as an example. No significant correlation was detected between η_o and Δr for any beach or bathymetric descriptor (Table V).

In order to gain a deeper understanding of the nature of the Δr, variability, the distances were finally correlated with the relative wave height, i.e., the ratio of the offshore H_{rms} over the water depth, H_{rms}/D (see Fig. 15 for an example of both beaches). Here, the water depth was computed including the measured sea surface level $D = \eta_o - z_b$. The obtained squared correlation coefficients were higher than those obtained previously

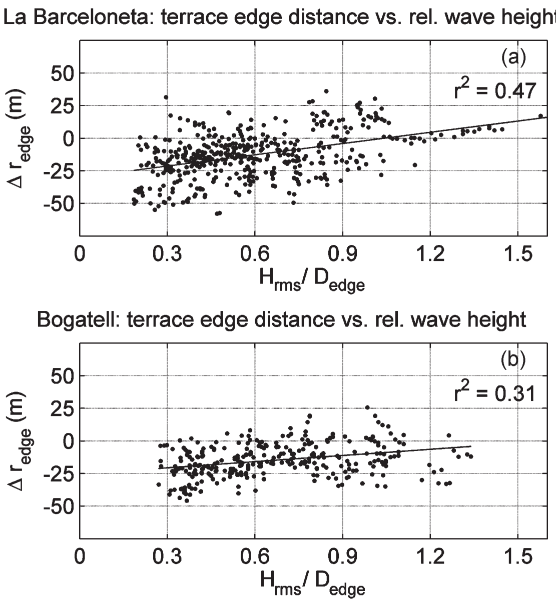

Fig. 15. Variation of $\Delta r_{\rm edge}$ with the offshore $H_{\rm rms}$ divided by the water depth $H_{\rm rms}/D_{\rm edge}$, at (a) La Barceloneta beach and at (b) Bogatell beach, for the valid profiles. Positive (negative) values of Δr indicate that the videoed bar position lies seaward (landward) of the real bar position.

(Table V). Thereby, this quantity (which includes the combined effects of $H_{\rm rms}$ and $D_{\rm edge}$) best explained the Δr variability.

VI. Discussion

The specific characteristics and conditions of Barcelona beaches differed significantly from the sites where similar methodological studies had been performed so far. The first distinctive property was the occurrence of a significant percentage of terraces (without a trough), implying the need for a descriptor of the bar location besides the location of minimum depth. Given the lack of a long-term averaged profile (a situation that can occur at many other sites), the proposed descriptor for the bar location was the slope break or terrace edge location $\boldsymbol{r_{edge}}$. As opposed to $\boldsymbol{r_{crest}}$, $\boldsymbol{r_{edge}}$ can be determined for both barred (with a trough) and terraced (without a trough) profiles.

Overall, the videoed barlines better reflected the location of $\boldsymbol{r_{crest}}$ (Table IV), making the use of $\boldsymbol{r_{crest}}$ favorable to compare with $\boldsymbol{r_{video}}$ if profiles are frequently barred (as occurs in la Barceloneta beach). In the case of predominance of terraced profiles (as occurs in Bogatell beach), videoed barlines are also a good proxy for the terrace edge position and can be used to study its dynamics. The bathymetric differences between the two studied beaches induced additional diversity in the behavior of the distances Δr: The predominantly shallow terraces in Bogatell-controlled wave breaking better than the deeper bars in La Barceloneta. In particular, the deepest bars in the latter beach were observed in 2003, and the corresponding videoed barlines were located up to 50 m landward of the real bar location. Aside from bathymetrical differences, the time-varying hydrodynamics resulted in further variations of Δr. The wave heights exhibited highly significant correlations with Δr, whereas the sea surface levels were uncorrelated to Δr. The obtained Δr best correlated with the ratio $H_{\rm rms}/D_{\rm edge}$, a descriptor that encompasses the influence of both the wave height and the water depth over the bar/terrace and that is commonly used to characterize depth-induced breaking.

A. Correction Methods for Reducing the Apparent Barline Variability

In Barcelona beaches, the apparent variability of Δr was mainly related to the changes in wave height and in the local profile shape. This variability should be preferably reduced before using the videoed barlines to analyze the real time evolution of the bars. Since we are mainly interested in evaluating the changes of bar position, reducing the average value of Δr is not essential. However, reducing the variability of Δr, quantified by $std(\Delta r)$, is desirable because it masks the real morphologic changes. The apparent variability induced by the differences in the local shape of the profiles (whether it is barred or terraced, the water depth over the bar/terrace, etc.) cannot be reduced because it would require detailed bathymetric information with a high temporal resolution, which is not available at our site (one annual bathymetric survey is performed at most). This fact also excludes correction methods based on model predictions of Δr because model results also depend strongly on the bathymetry [8].

On the other hand, it would be desirable to find a method to diminish the apparent variability based on hydrodynamic information only. In particular, the highly significant correlation detected between Δr and $H_{\rm rms}$ (Figs. 12 and 13) indicated that a proportion of the $H_{\rm rms}$-induced variability might be reduced. Two potential empirical correction methods were hereby tested to reduce the apparent barline migration due to $H_{\rm rms}$ variability. The first method involved using the best fit lines obtained in Table V to normalize the barline locations to a standard $H_{\rm rms}$ value. The second method involved selecting the barlines sampled at a specific range of $H_{\rm rms}$. Different possible ranges of $H_{\rm rms}$ were tested, keeping in mind both the reduction of $std(\Delta r)$ (a measure of the apparent variability) and the probability of the $H_{\rm rms}$ range occurring in Barcelona. The latter was evaluated with the time percentage (TP) during which $H_{\rm rms}$ occurred within a specific range during the study period. The smallest the TP value, the least amount of sampled barlines would be available to track the real bar dynamics.

Table VI shows the results of both correction methods, including the obtained $std(\Delta r)$ after the correction and the number of Δr that remained, N. The first method was not very efficient, giving a limited reduction of $std(\Delta r)$, ranging from 2% to 6% (depending on the beach and the morphologic descriptor). The largest reduction was obtained in La Barceloneta when using $\boldsymbol{r_{crest}}$, which corresponds with the regression analysis yielding the best correlation (Table V). In theory, this method might provide a better reduction if the analysis was performed for shorter time periods (for instance, for one single bathymetry). When the latter was performed, however, the limited number of barlines per bathymetry resulted in insignificant squared correlation coefficients between Δr and $H_{\rm rms}$ in most of the cases. In particular, significant correlations were only obtained for the two bathymetries of La Barceloneta in 2003 and the bathymetry of Bogatell in 2005. In addition,

TABLE VI
STANDARD DEVIATION OF THE DISTANCES AFTER APPLYING DIFFERENT CORRECTION METHODS

		La Barceloneta (using r_{edge})		La Barceloneta (using r_{crest})		Bogatell (using r_{edge})		Bogatell (using r_{crest})	
Method of correction to reduce Δr variability	***TP***	***N***	***std(Δr) (m)***	***N***	***std(Δr) (m)***	***N***	***std(Δr) (m)***	***N***	***std(Δr (m))***
No correction ($0.5<H_{rms}<3$m)	*26.2%*	*468*	*17.6*	*415*	*15.6*	*326*	*13.0*	*152*	*10.0*
H_{rms} correction 1: using best fit lines ($0.5<H_{rms}<3$m)	*26.2%*	*468*	*16.7*	*415*	*14.7*	*326*	*12.7*	*152*	*9.7*
H_{rms} correction 2a: selecting barlines for $0.5<H_{rms}<1.25$m	*23.7%*	*287*	*15.5*	*259*	*14.2*	*200*	*11.4*	*119*	*10.1*
H_{rms} correction 2b: selecting barlines for $0.75<H_{rms}<1.5$m	*10.3%*	*222*	*15.4*	*198*	*14.1*	*207*	*11.9*	*104*	*10.1*
H_{rms} correction 2c: selecting barlines for $1.0<H_{rms}<1.75$m	*4.1%*	*154*	*14.5*	*136*	*13.1*	*146*	*10.7*	*61*	*10.5*

Here, N is the number of distances that remained after the correction and TP refers to the time percentage during which H_{rms} occurred within the corresponding range during the study period.

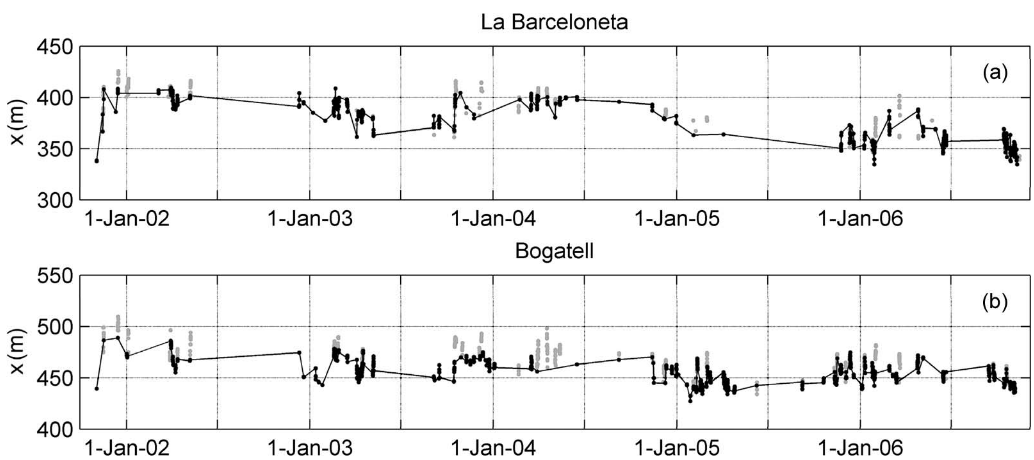

Fig. 16. Time series of the cross-shore position of the alongshore averaged barlines during the study period in (a) La Barceloneta and in (b) Bogatell. The gray dots indicate all the barlines and the black dots correspond to the selected barlines sampled with $0.75 < H_{\rm rms} < 1.5$ m in La Barceloneta and with $0.5 < H_{\rm rms} < 1.25$ m in Bogatell.

even in these cases, the result of the first correction method did not improve significantly. Moreover, a limitation of this latter approach would again be the need for bathymetric measurements every few months.

The second correction method, based on a selection of barlines sampled at certain $H_{\rm rms}$, is not only simpler (it does not require bathymetric surveys) but also further reduces the $std(\Delta r)$. For instance, when we used a range with the smallest $H_{\rm rms}$ that still allows for barline detection ($0.5 < H_{\rm rms} < 1.25$ m), and comparing with $\boldsymbol{r_{edge}}$, a 12% reduction was obtained in the two beaches, with $std(\Delta r)$ reaching a value of 15.5 m in La Barceloneta and 11.4 m in Bogatell. When comparing with $\boldsymbol{r_{crest}}$ in La Barceloneta, a reduction of 9% was obtained, reaching a value of $std(\Delta r)$ of 14.2 m. Using this (smallest) range of $H_{\rm rms}$, the TP did not change significantly compared to the TP of the total $H_{\rm rms}$ range that can be used for bar sampling with the specific conditions of Barcelona site ($0.5 < H_{\rm rms} < 3.0$ m, explained in Section III-B). The reduction in $std(\Delta r)$ was very similar when using other ranges with 0.75 m of variation of $H_{\rm rms}$, being slightly largest for higher $H_{\rm rms}$ values. However, using ranges of larger $H_{\rm rms}$ values at the Barcelona site significantly reduces the probability of the occurrence of $H_{\rm rms}$, allowing a smaller amount of available barlines for tracking the real bar changes. For instance, $std(\Delta r_{\rm crest})$ in La Barceloneta was reduced to 13.1 m when using the range $1.0 < H_{\rm rms} < 1.75$ m, but TP decreased to 4.1% (Table VI).

From this analysis, the second method arises as a simpler and more efficient way to reduce $H_{\rm rms}$-induced barline variability. In Bogatell, the recommended specific range of $H_{\rm rms}$ would be $0.5 < H_{\rm rms} < 1.25$ m (method 2a in Table VI). However, in La Barceloneta, the range could also be $0.75 < H_{\rm rms} < 1.5$ m, specially bearing in mind that bars can be located in deeper areas, requiring larger wave heights to break on them. As an example of the application of this second correction method, Fig. 16 shows the time series of the cross-shore position of the alongshore averaged barlines sampled in La Barceloneta and Bogatell during the study period. The gray dots indicate all the possible barlines and the black dots indicate the selected barlines sampled in the ranges recommended above. The qualitative effect of the reduction of $std(\Delta r)$ can be clearly appreciated and the real evolution of the bars becomes more evident.

Several sources of error can explain the remaining variability of the cross-shore distances (11 m in Bogatell and 14 m in La Barceloneta). The cross-shore induced noise due to image resolution is of 1.5 m at most and can only explain a small percentage of this remaining variability. Pixel signal saturation can also induce errors in the detection of the maximum intensity lines, as shown by [18]. However, the latter study also indicated that the percentage of saturated pixels was generally smaller than 5%. The two most important sources of error are the variability of the profile shapes and the remaining variability of the wave height (which is of 0.75 m after applying the correction method).

B. Comparison With Other Sites

The sites where a similar methodological analysis was available in the literature (Duck, Egmond, and Tairua beaches, see Table I) were significantly different from the beaches of this paper. First, the presence of a bar with a distinct trough in all the bathymetric profiles was assumed in the previous studies, whereas only 53% of the Barcelona profiles verified this condition. Some 20% of the Barcelona profiles were terraced (without a trough) and the rest was considered to be featureless. Despite these differences, the distances Δr between videoed and real bar positions in Barcelona beaches were similar to those measured at other sites (compare Tables I and V). For instance, maximum negative distances were similar to those detected at Duck Beach [7], with a similar tendency of Δr to increase as the bar was located at larger water depths. In addition, x_{edge} and x_{crest} were both correlated with x_{video} at the 99% confidence level, like in most of the other sites.

Second, the most distinctive difference of the present study site with respect to the previous ones is the variability of the sea surface level η_o which is much smaller than at Duck, Egmond, and Tairua. During barline detection, the η_o only changed some 0.5 m at our site, whereas it varied some 1.5 m in the previous studies. In contrast to all these previous studies, no significant correlation was detected between Δr and η_o in Barcelona beaches. On the other hand, these almost tideless conditions made Barcelona beaches to be a perfect laboratory for testing the H_{rms}-induced variability of Δr. A highly significant positive correlation between Δr and H_{rms} was found at our site, whereas no significant correlation between these two quantities was detected in the previous sites [6], [8]. A tendency for the distances to increase for increasing wave heights was reproduced with model simulations by [6] but only for a certain range of H_{rms} (up to 2 m). The distances they measured in Egmond did not show the corresponding correlation with H_{rms}. Plant and Holman [7] even mentioned that the distances had a slight tendency to decrease for larger wave heights in Duck and reference [9] also detected a negative correlation between these two quantities in Tairua beach. This negative correlation is difficult to interpret from a physical point of view, corresponding to the fact that none of these correlations were significant at the 95% level (Table I). At the beaches with important tidal oscillations, the clear and strong η_o-induced barline variability may partially obscure the effect of H_{rms} changes.

The stochastic nature of H_{rms} is very different from the cyclic behavior of η_o, and this affected the applicability of correction methods and the corresponding results. For instance, the practical smoothing method to reduce barline variability used by [8] was not applicable at our site due to the absence of a cyclic behavior in H_{rms} variability. The first method implemented in this paper was applied similarly in the tidal dominated Egmond beach to reduce the η_o-induced variability in Δr [6]. They obtained a more significant reduction (up to 50%), linked to the fact that the correlation between Δr and η_o was more significant. They also proposed a simpler reduction method, which they recommended in the lack of bathymetric surveys, similar to our second method. By selecting the barlines sampled during low tide, they obtained reductions of the $std(\Delta r)$ of some 10%, reaching a value of 8 m. The relative reduction obtained in Barcelona with the second method was also of the order of 10% and the final values of $std(\Delta r)$ (11 m in Bogatell and 14 m in La Barceloneta) were of the same order.

VII. Conclusion

The suitability of using video imaging to study the dynamics of nearshore sandbars in the tideless beaches of Barcelona has been assessed, determining the limitations of this methodology and the corresponding errors in data acquisition involved. This paper is particularly relevant due to the critical differences in wave and tide conditions and in bathymetric characteristics between the Barcelona site and the other beaches where similar methodological analyses have been performed.

A preliminary step prior to comparing videoed barline with real bar positions was to characterize the shape of the available bathymetric profiles, in order to subsequently study how this shape influenced the barline detection from video-images. In order to characterize the morphologic bar position, together with the bar crest position we used the location of the terrace edge or slope break, defined as the location with the maximum slope change (equivalent to the maximum perturbation point of the profile). This descriptor can be used in case of barred and terraced profiles, and it does not require a long-term averaged profile. A tool to differentiate between terraced profiles and featureless profiles was also applied successfully to the beach profile data, the terraces being distinguished by a large magnitude of the slope break and a small terrace slope. Bogatell beach showed a significant occurrence of pure terraces (in more than 50% of the profiles), the remaining profiles being barred (some 40%). In La Barceloneta, the majority of the profiles were barred (almost 60%) and the rest were featureless (some 30%, located in the north), with a limited presence of terraces.

In the Barcelona beaches, the videoed barlines reflected the location of the bar crest (only evaluated in case of bar presence) slightly better than the location of the terrace edge, although the two morphologic descriptors were highly correlated with the videoed position. However, in Bogatell, this result was masked by the small amount of data available when using the bar crest descriptor, making the use of the terrace edge position recommendable for comparison with the videoed barlines at this beach.

The distances between videoed barlines and real bar/terrace position, Δr, were of the order of 10 m, with maximum discrepancies of 50 m. The bathymetric differences in the cross-shore profiles induced different deviations of the videoed barlines. A more distinct bar/terrace, located in shallower water, had more control over the location of wave breaking, decreasing the variability of the cross-shore positions of the barlines for varying wave heights. A significant percentage of waves propagated without breaking over the bars located in depths larger than 2 m (found in 2003 at La Barceloneta), giving a larger Δr variability. The distances between the videoed and the real bar positions showed a highly significant positive correlation with the root-mean-squared wave height $H_{\rm rms}$. The smallest deviations between barlines and the actual bar position were found for the largest wave heights. In contrast with all the previous studies, no significant correlation was detected between Δr and the sea surface level. The quantity that best explained the Δr variability was the ratio of $H_{\rm rms}$ to the water depth over the bar/terrace.

The linear relationship between Δr and $H_{\rm rms}$ indicated a potential method for correcting the complete data set of videoed barlines with respect to the $H_{\rm rms}$ present during the sampling period. However, this step must be taken carefully since the actual shape of the bathymetric profiles, which is generally unknown, also affects the relationship between Δr and $H_{\rm rms}$. The most suitable method to reduce $H_{\rm rms}$-induced variability proved to be the use of the barlines sampled in a certain range of $H_{\rm rms}$ (it reduced the $std(\Delta r)$ by 10%). In Bogatell, using barlines sampled with $0.5 < H_{\rm rms} < 1.25$ m reduced the Δr variability to 11 m. In La Barceloneta, the recommended range was $0.75 < H_{\rm rms} < 1.5$ m (since the bar was often located at larger water depths), obtaining values of Δr variability of 14 m.

This paper shows that, when only video data are available at Barcelona beaches, the videoed barlines can be used to study the dynamics of bar crests or terrace edges, sampling barlines within the proposed ranges of $H_{\rm rms}$ and bearing in mind the remaining uncertainty. The methodological approach developed here could be employed in other sites with frequent presence of terraced profiles. Moreover, the described calibration for barline extraction in the Barcelona beaches could also be useful for sites with similar tideless hydrodynamic characteristics.

Acknowledgment

The authors would like to thank O. Chic for helping with the data acquisition, Dr. G. Ruessink for providing the software for barline acquisition, and Dr. T. Mendoza for helping with the map in Fig. 2. Wave and tide data were provided by "Puertos del Estado" from the Spanish government. Video and bathymetric data were provided by the Coastal Ocean Observatory, Institut de Ciències del Mar, Consejo Superior de Investigaciones Cientificas, Barcelona, Spain. The authors would also like to thank Dr. M. C. Haller and two other anonymous reviewers for their comments.

References

[1] K. T. Holland, R. A. Holman, T. C. Lippmann, J. Stanley, and N. Plant, "Practical use of video imagery in nearshore oceanographic field studies," *IEEE J. Ocean. Eng.*, vol. 22, no. 1, pp. 81–92, Jan. 1997.

[2] R. A. Holman and J. Stanley, "The history and technical capabilities of Argus," *Coastal Eng.*, vol. 54, no. 6/7, pp. 447–491, Jun./Jul. 2007.

[3] I. M. J. van Enckevort, B. G. Ruessink, G. Coco, K. Suzuki, I. L. Turner, N. G. Plant, and R. A. Holman, "Observations of nearshore crescentic sandbars," *J. Geophys. Res.*, vol. 109, no. C6, p. C06 028, Jun. 2004. DOI: 10.1029/2003JC002214.

[4] A. Kroon, "Sediment transport and morphodynamics of the beach and nearshore zone near Egmond, The Netherlands," Ph.D. dissertation, Utrecht Univ., Utrecht, The Netherlands, 1994.

[5] T. C. Lippmann and R. A. Holman, "Quantification of sand bar morphology: A video technique based on wave dissipation," *J. Geophys. Res.*, vol. 94, no. C1, pp. 995–1011, Jan. 1989.

[6] I. M. J. van Enckevort and B. G. Ruessink, "Effect of hydrodynamics and bathymetry on video estimates of nearshore sandbar position," *J. Geophys. Res.*, vol. 106, no. C8, pp. 16 969–16 979, 2001.

[7] N. G. Plant and R. A. Holman, "Extracting morphologic information from field data," in *Proc. 26th Int. Conf. Coastal Eng.*, 1998, pp. 2773–2784.

[8] B. G. Ruessink, P. S. Bell, I. M. J. van Enckevort, and S. G. J. Aarninkhof, "Nearshore bar crest location quantified from time-averaged X-band radar images," *Coastal Eng.*, vol. 45, no. 1, pp. 19–32, Mar. 2002.

[9] K. R. Bryan and A. Swales, "Inferring bar position from video imagery of breaking waves at Tairua Beach, New Zealand," presented at the Coasts and Ports Australasian Conf., 2003, Paper 20.

[10] K. S. Kingston, B. G. Ruessink, I. M. J. van Enckevort, and M. A. Davidson, "Artificial neural network correction of remotely sensed sandbar correction," *Mar. Geol.*, vol. 169, no. 1, pp. 137–160, Sep. 2000.

[11] P. S. Alexander and R. A. Holman, "Quantification of nearshore morphology based on video imaging," *Mar. Geol.*, vol. 208, no. 1, pp. 101–111, Jul. 2004.

[12] L. Pape, B. G. Ruessink, M. A. Wiering, and I. L. Turner, "Recurrent neural network modeling of nearshore sandbar behaviour," *Neural Netw.*, vol. 20, no. 4, pp. 509–518, May 2007.

[13] S. G. J. Aarninkhof and B. G. Ruessink, "Video observations and model predictions of depth-induced wave dissipation," *IEEE Trans. Geosci. Remote Sens.*, vol. 42, no. 11, pp. 2612–2622, Nov. 2004.

[14] A. van Dongeren, N. Plant, A. Cohen, D. Roelvink, M. C. Haller, and P. Catalán, "Beach wizard: Nearshore bathymetry estimation through assimilation of model computations and remote observations," *Coastal Eng.*, vol. 55, no. 12, pp. 1016–1027, Dec. 2008.

[15] K. D. Splinter and R. A. Holman, "Bathymetry estimation from single-frame images of nearshore waves," *IEEE Trans. Geosci. Remote Sens.*, vol. 47, no. 9, pp. 3151–3160, Sep. 2009.

[16] E. Ojeda and J. Guillén, "Shoreline dynamics and beach rotation of artificial embayed beaches," *Mar. Geol.*, vol. 253, no. 1/2, pp. 51–62, Jul. 2008.

[17] E. Ojeda and J. Guillén, "Monitoring beach nourishment based on detailed observations with video measurements," *J. Coastal Res.*, vol. SI-48, pp. 100–106, 2006.

[18] M. C. Haller and P. A. Catalán, "Remote sensing of wave roller lengths in the laboratory," *J. Geophys. Res.*, vol. 114, no. C7, p. C07 022, Jul. 2009.

Francesca Ribas received the B.S. degree in physics from the Universitat de Barcelona, Barcelona, Spain, in 1998 and the Ph.D. degree from the Universitat Politècnica de Catalunya, Barcelona, in 2004.

She held postdoctoral contracts with Utrecht University, Utrecht, The Netherlands, in 2004 and with the Institut de Ciències del Mar, Barcelona, in 2005–2007. She is currently an Assistant Professor with the Universitat Politècnica de Catalunya. Her current research interests include the application of numerical modeling and optical remote sensing to understand the dynamics of the nearshore.

Elena Ojeda received the B.S. degree in ocean sciences from the Universidad de Las Palmas de Gran Canaria, Las Palmas de Gran Canaria, Spain, in 2002 and the Ph.D. degree from the Universitat Politècnica de Catalunya, Barcelona, Spain, in 2009.

She is currently working as a Researcher with the Institut de Ciències del Mar, Barcelona. Her research interests are the monitoring of morphodynamic descriptors using remote sensing techniques and *in situ* measurements.

Timothy D. Price received the M.Sc. degree in physical geography from Utrecht University, Utrecht, The Netherlands, in 2007, where he is currently working toward the Ph.D. degree, focusing on the behavior of crescentic sandbars.

As part of his M.Sc. degree, he spent six months with the Institut de Ciències del Mar, Barcelona, Spain. His research includes the integration of nearshore video images into numerical simulation models of sandbar morphodynamics.

Jorge Guillén received the B.S. degree in geology from the Universitat de Barcelona, Barcelona, Spain, in 1983 and the Ph.D. degree in marine sciences from the Universitat Politècnica de Catalunya, Barcelona, in 1992.

He is currently a Scientific Researcher with the Institut de Ciències del Mar, Barcelona. Main topics of his research are sediment dynamics in shallow waters and morphodynamics and coastal evolution under different timescales using both *in situ* and remote observations.

Dr. Guillén manages the Coastal Marine Station of Barcelona.